Impact of UV- and carbodiimide-based crosslinking on the integrin-binding properties of collagen-based materials

Short title: Integrin binding to UV- and carbodiimide-crosslinked collagen

Daniel V. Bax[1,2*], Natalia Davidenko[1], Samir W. Hamaia[2], Richard W. Farndale[2], Serena M. Best[1], Ruth E. Cameron[1]

[1] Department of Materials Science and Metallurgy, University of Cambridge, 27 Charles Babbage Road, Cambridge, CB3 0FS, United Kingdom

[2] Department of Biochemistry, University of Cambridge, Downing Site, Cambridge, CB2 1QW, United Kingdom

*Corresponding author. Tel: +44 (0)1223 334560; fax: +44 (0)1223 334567.

E-mail address: dvb24@cam.ac.uk

Keywords: cell adhesion, integrin binding, collagen, UV crosslinking

Abstract

Collagen constructs are widely used for tissue engineering. These are frequently chemically crosslinked, using EDC, to improve their stability and tailor their physical properties. Although generally biocompatible, chemical crosslinking can modify crucial amino acid side chains, such as glutamic acid, that are involved in integrin-mediated cell adhesion. Instead UV crosslinking modifies aromatic side chains. Here we elucidate the impact that EDC, in combination with UV, exerts on the activity of integrin-binding motifs. By employing a model cell line that exclusively utilises integrin $\alpha_2\beta_1$, we found that whilst EDC crosslinking modulated cell binding, from cation-dependent to cation-independent, UV-mediated crosslinking preserved native-like cell binding, proliferation and surface colonisation. Similar results were observed using a purified recombinant I-domain from integrin α_1. Conversely, binding of the I-domain from integrin α_2 was sensitive to UV, particularly at low EDC concentrations. Therefore, from this *in vitro* study, it appears that UV can be used to augment EDC whist retaining a specific subset of integrin-binding motifs in the native collagen molecule. These findings, delineating the EDC- and UV-susceptibility of cell-binding motifs, permit controlled cell adhesion to collagen-based materials through specific integrin ligation *in vitro*. However, *in vivo*, further consideration of the potential response to UV wavelength and dose is required in the light of literature reports that UV initiated collagen scission may lead to an adverse inflammatory response.

Graphical Abstract

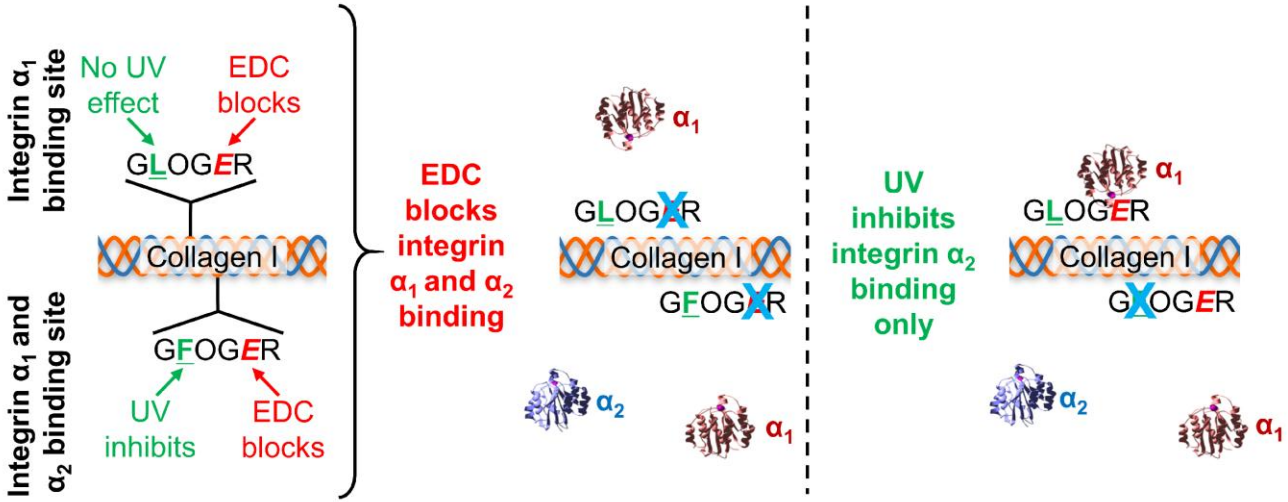

1. Introduction

The aim of tissue engineering is the recreation of tissue via physical supports that act as guides for the distribution and bio-activity of cells [1,2]. In tissues it is the extracellular matrix (ECM), surrounding cells, that inherently performs this function. As such, purified ECM components have gained popularity in recent years for scaffold fabrication. These ECM components comprise proteins, glycoprotiens and glycosaminaoglycans which, together, form the cell niche and determine the cellular phenotype. Of these ECM components, there has been particular interest in fibrillar collagen I, due to its abundance and wide tissue distribution [3]. Collagen is a triple helical protein which bestows physical strength, and stiffness, to tissue engineered constructs [4]. Additionally, collagen adheres to a diverse range of cell types through well-characterised cell binding motifs [5]. Combined with low cost and high purity, collagen I has become the precursor of choice for biomaterials fabrication.

Many of the crosslinks found in native collagen are disrupted during purification, necessitating chemical or physical crosslinking. This ensures appropriate durability of the collagen-based material. Numerous physical crosslinking process have been developed [6–9], however many of these are not suitable for collagen-based materials due to their tendency to heat, and so thermally denature, the collagen molecules. By contrast, chemical crosslinking can preserve the collagen molecular folding. For example carbodiimide chemical crosslinking using 1-ethyl-3-(3-dimethylaminopropyl-carbodiimide hydrochloride (EDC) in the presence of N-hydroxy-succinimide (NHS) is frequently used for collagen-based materials stabilization [10]. This process forms a ‘zero-length’ amide bond between carboxylate groups (for example on aspartic acid or glutamic acid residues) and adjacent primary amines (for example on lysine residues). A major advantage of this treatment is non-toxicity, since neither EDC nor NHS are

incorporated into the material and are easily removed by washing [11–14]. Careful control over the crosslinking parameters allows refinement of the mechanical properties and degradation kinetics of the resultant scaffold [10,15]. This has identified the often-used crosslinking conditions of 11.5 mg/mL EDC in the presence of 2.76 mg/mL NHS as an optimal crosslinking strategy (referred to as 100% throughout this paper). The stoichiometry of this reaction dictates that there is a 5-fold molar excess of EDC relative to carboxylate groups on collagen, implying that the carboxylate content of the collagen-based material is depleted [10]. This is of particular interest as Gxx′GEx″ cell adhesive motifs in collagen contain a critical carboxylic acid group [16]. These motifs bind through cell-surface integrins, a major class of heterodimeric cell adhesion receptor. Of the 24 different integrin heterodimers [17], integrins $\alpha_1\beta_1$, $\alpha_2\beta_1$, $\alpha_{10}\beta_1$, and $\alpha_{11}\beta_1$ are collagen binding [18]. Each of the Gxx′GEx″ motifs possesses differing affinity for each integrin. This is dictated by the amino acid at the x position, which may be phenylalanine (F), leucine (L), arginine (R), or methionine (M) [5]. These motifs bind to an inserted A-domain (I-domain) within the α subunit of the integrin. As such it is the I-domain that bestows the collagen-cell-binding motif specificity to the integrin. The crystal structure of the I-domain-collagen interaction shows that the carboxylate group on the E residue of the Gxx′GEx″ motifs is critical for coordination with a Mg^{2+} ion within the I-domain [19]. This free carboxylate group within the integrin-binding motifs is the same chemical group that is chemically modified by EDC crosslinking [13].

EDC-attributed loss of native cell attachment has been highlighted recently where Mg^{2+}-dependent integrin mediated adhesion is lost and is replaced by Mg^{2+}-independent adhesion [20]. This resulted in consummate depletion of cell proliferation on EDC-crosslinked collagen. The use of lower chemical crosslinking concentrations represents

one strategy to minimize the impact of EDC crosslinking on the cell-biological activity. For example a 10-fold dilution in EDC crosslinking could restore the cellular response to near non-crosslinked controls [10,20]. This raises an intriguing conundrum for biomaterials design where the requirement for physical attributes, such as stability and mechanical properties, are balanced by the desire to retain the native biological activity of the collagen precursors. To overcome this dilemma we have proposed the use of multiple, low dose crosslinking strategies [21]. The premise behind this approach is that each crosslinking process modifies a small proportion of susceptible groups. By utilizing different crosslinking strategies, each of which targets a different chemical group of collagen, we hypothesize that sufficient groups can be retained to maintain bio-activity, whilst simultaneously accumulating sufficient chemical bonds to yield appropriate physical properties [21].

One such approach includes the use of low dose EDC crosslinking in combination with low dose UV irradiation a short wavelength (254 nm). As previously described, low dose EDC crosslinking modifies a sufficiently low proportion of the carboxylate side groups to retain bioactivity. UV, by comparison, predominantly modifies aromatic side chains such as tyrosine and phenylalanine [22–24]. Therefore, UV supplementation of low-dose EDC crosslinking offers the potential to crosslink protein molecules without ablating an overwhelming majority of the acidic or basic side chains that are critical for cell recognition. Furthermore, UV offers numerous additional advantages such as avoiding the need for toxic chemicals, ease of treatment and sterility [25]. However, these need to be balanced against potential collagen denaturation and fragmentation [26,27] that could lead to the release of pro-inflammatory peptides [28,29]. UV crosslinking of collagen scaffolds showed improved physical properties and does not adversely affect cell ligation [21]. Despite this, the mechanism of cellular

interaction with collagen treated using a UV augmented, low-dose EDC crosslinking regime is unknown. As such, this paper seeks to define the impact that EDC crosslinking, in combination with UV irradiation, has on the integrin-binding properties of collagen–based materials, and in turn, on cellular adhesion and proliferation. As collagen is widely used as a precursor for a plethora of biomaterials applications this analysis provides important new information on the use of combined crosslinking approaches for tailored cell engagement with biomaterials.

2. Materials and Methods

2.1. Materials

Bovine Achilles tendon insoluble type I collagen (C4387) was obtained from Sigma Aldrich, UK. HT1080 cells, derived from a human fibrosarcoma, were from the European Collection of Animal Cell Cultures, Porton Down, UK. Unless stated otherwise all other reagents were from Sigma-Aldrich, UK.

2.2. Amino acid analysis

~1mg of collagen I was subjected to amino acid analysis (Department of Biochemistry, University of Cambridge, UK). The content of each amino acid was corrected against a norleucine standard and then divided by the total content of all measured amino acids. Cystine and tryptophan were excluded due to degradation during analysis, however they are absent in collagen. The predicted amino acid content was calculated from the primary amino acid sequences of the bovine collagen alpha I (I) (UniProtKB-P02453) and bovine collagen alpha 2 (I) chains (UniProtKB-P02465).

2.3. Film preparation

Collagen was swollen as a 0.5% (w/v) suspension in 50 mM acetic acid at 4^{o}C overnight before homogenising on ice for 20 min at 13500 rpm using an Ultra-Turrax VD125 (VWR International Ltd., UK) homogeniser. This was centrifuged at 2500 rpm for 5 min. (Hermle Z300, Labortechnik, Germany) to remove air bubbles before pipetting 100 μL of the slurry/well into Immulon-2HB 96-well plates (Thermo Scientific). These were dried for 48 h in a laminar flow cabinet to produce uniform ~8 μm thick films, containing 0.5mg of collagen I that covered the entire well surface area.

Chemical crosslinking was performed using EDC/NHS at molar ratio of 5 EDC / 2 NHS for each COO^- group on collagen. 100% crosslinking solution contained 1.15 g EDC, 0.276 g NHS in 200 ml 75 % (v/v) ethanol as the standard (100 % - 30mM EDC) crosslinking condition. The crosslinking solution was varied by dissolving increased amounts of EDC/NHS in 75 % ethanol to produce a higher EDC/NHS concentration relative to the COO^- groups on collagen or, by diluting the 100 % solution with 75 % ethanol to the appropriate concentration. Non-crosslinked (0 % EDC/NHS) films were incubated in 75 % ethanol in the absence of EDC/NHS. Films were crosslinked at room temperature for 2 h after which the films were washed extensively with deionised water and dried in a laminar flow cabinet for 48 h at room temperature.

The EDC/NHS films were UV crosslinked by irradiating at a wavelength of 254 nm for 30 min in a UVP UV Crosslinker (CL-1000 Series, Ultra-Violet Products Ltd., UK). The intensity was set to either 0.42 or 0.96 J/cm^2.

2.4. Attenuated total reflectance-Fourier-transform infrared spectroscopy (ATR-FTIR)

ATR-FTIR spectra were obtained using a Bruker Tensor 27 FTIR fitted with a diamond ATR accessory. Spectra were obtained between 500 and 4000 cm^{-1} with a resolution of 2 cm^{-1}.

2.5. Platelet adhesion

Non-specific platelet adsorption to the well was blocked with 5 % (w/v) bovine serum albumin (BSA) in phosphate buffered saline (PBS) for 60 min at room temperature. This was aspirated, and the wells washed three times with PBS. Platelet-rich plasma, pooled from 4 donors, was provided by the National Health Service Blood

and Transplants (NHSBT) authority and used in accordance with the Declaration of Helsinki. Platelets were prepared from platelet-rich plasma by centrifugation for 15 min, 240 g and the pellet discarded. 1 μL of Prostaglandin E_1 (100 μg/mL in ethanol) was added per mL of platelet supernatant to prevent platelet aggregation. This suspension was centrifuged at 640 g for 10 min to sediment the platelets. These were subsequently resuspended in Tyrodes buffer (140 mM NaCl, 5.6 mM Glucose, 2 mM $MgCl_2$, 0.4 mM NaH_2PO_4, 12 mM $NaHCO_3$, 2.7 mM KCl, 10 mM HEPES pH 7.4) to a density of $1x10^8$ /mL. $MgCl_2$ or EDTA was added to a final concentration of 5 mM then 100 μL of platelet suspension was added to the wells and incubated at room temperature for 30 min to allow platelet attachment to the collagen films. Loosely bound platelets were removed by washing 3 x 200 μL with Tyrodes. Bound platelets were detected by adding 150 μL of lysis buffer containing a p-nitrophenyl phosphate (PNP) substrate (81mM TriSodium Citrate, 31mM Citric Acid, 0.1% v/v Triton X-100, 1.85 mg/mL PNP substrate, pH 5.4). Following a 90 min incubation at room temperature, 100 μL of 2M NaOH was added and the absorbance read at 405 nm (A_{405}) using a Fluostar Optima plate reader (BMG Labtech).

2.6. HT1080 cell adhesion analysis

HT1080 cells were routinely cultured in complete media (Dulbecco's modified Eagle's medium (DMEM) containing 10 % (v/v) fetal bovine serum and 1 % (v/v) streptomycin/penicillin) in a humidified incubator with 5% CO_2 at 37 °C, passaging 1:10 every 3-4 days. Cells layers at ~75 % confluence were prepared for analysis by detaching with 0.05 % (w/v) trypsin / 0.02 % (w/v) EDTA, centrifuging at 160 g for 3 min, then re-suspending in serum free DMEM at a density of $5x10^5$ cells/mL. $MgCl_2$ or EDTA were added to a final concentration of 5 mM. Non-specific HT1080 cell

adsorption to the well plate was BSA blocked as for platelet adhesion analysis and then 100 μL of cells was added for 45 min at 37 °C / 5 % CO_2. Loosely-bound cells were removed with 3 x 200 μL PBS washes and the bound cells were then measured using the PNP substrate as for platelet adhesion.

2.7. HT1080 cell spreading analysis

Collagen films were BSA blocked as for platelet adhesion and the cells were prepared as for HT1080 cell adhesion analysis, except that the cells were resuspended in complete media to a density of $1x10^4$ cells/mL. After 24 h at 37 °C / 5 % CO_2 the cells were fixed by adding 37% (w/v) formaldehyde directly to the cell media to a final concentration of 3.7% (w/v) for 20 min at room temperature. The wells were washed with PBS then images were taken on a LEICA DMI6000CS phase contrast microscope fitted with a LEICA DFC340FX camera at 20 X magnification. The cell area was quantified in Image J by manually tracking the cell periphery.

2.8. Integrin I domain binding analysis

The collagen binding I-domains from integrin α_1 and α_2 subunits were expressed in *E. coli* and purified in-house as glutathione S transferase (GST) tagged recombinant proteins as described in [30]. Non-specific adsorption was blocked with 5% (w/v) BSA in binding buffer (50 mM TRIS, 140 mM NaCl, 1 mg/mL BSA, pH 7.4) for 60 min at room temperature. The samples were washed 3 x 200 μL binding buffer then 5 μg/mL recombinant integrin α_1 or α_2 I domain in binding buffer containing either 5 mM $MgCl_2$ or 5 mM EDTA was added for 60 min at room temperature. The samples were washed 3 x 200 μL binding buffer containing 5 mM $MgCl_2$ or 5 mM EDTA respectively. I-domain binding was quantified through the presence of the GST tag by using 100 μL of

1:10,000 diluted horseradish peroxidise (HRP)-conjugated goat anti-GST antibody (Life Technologies) for 20 min at room temperature. The antibody was aspirated, and the films washed 4 x 200 μL binding buffer containing either 5 mM $MgCl_2$ or 5 mM EDTA for 20 min each wash. 100 μL of 3,3',5,5'-Tetramethylbenzidine (TMB) substrate (Thermo Scientific) was added to each well and, once the reaction had attained a blue colour, the reaction was terminated with 100 μL of 2.5 M H_2SO_4. The absorbance at 450 nm (A_{450}) was then measured using a Fluostar Optima plate reader (BMG Labtech). Negative control no-I-domain values were deducted from all values.

2.9. HT1080 growth

Non-specific binding was BSA blocked as for platelet adhesion analysis and the cells were prepared as for HT1080 cell adhesion analysis except that they were suspended at a density of $1x10^4$ cell/mL in complete media. 200 μL of HT1080 cells were added to the films for either 1, 2, or 4 days in a humidified incubator at 37 °C / 5 % CO_2. At each time point the cells were fixed by adding 37% (w/v) formaldehyde directly to the media to a final concentration of 3.7 % (w/v). After 20 min at room temperature the samples were washed 3 x PBS. The number of cells per field of view was counted manually using a LEICA DMI6000CS phase contrast microscope fitted with a LEICA DFC340FX camera at 20X magnification.

2.10. HT1080 surface coverage

The wells were BSA blocked and cell seeded as for HT1080 cell growth. After 4 days in culture the cell layer was fixed by adding 37% (w/v) formaldehyde to a final concentration of 3.7 % (w/v). The samples were washed 3 x PBS then images taken on a LEICA DMI6000CS phase contrast microscope fitted with a LEICA DFC340FX

camera at 20X magnification. The cell-occupied surface area of triplicate samples was calculated using manual tracking in Image J.

2.11. Statistical analysis

Unless otherwise stated all values represent means of quadruplicate or triplicate measurements ± standard deviations from the mean. Statistical significance was determined with a student t-test with unequal variance where N/S indicates $p>0.05$, * indicates $p\leq0.05$, ** indicates $p\leq0.01$, *** indicates $p\leq0.001$ and **** indicates $p\leq0.0001$.

3. Results

3.1. Influence of EDC/NHS and UV on integrin α_2-dependent platelet adhesion to collagen-based films.

We have previously shown that UV irradiation can be used to improve the stability of collagen based materials [21], which in-turn may be used to augment a low EDC crosslinking condition. To date the cellular response to this combined crosslinking approach is unknown. Platelets were chosen as a model system as they utilise integrin $\alpha_2\beta_1$ as the sole collagen-binding integrin [31,32]. This allows examination of a single collagen binding integrin which is not possible with cells that contain multiple collagen-binding receptors (Figure 1). In the absence of UV crosslinking, platelet adhesion was highly sensitive to the degree of EDC/NHS crosslinking. In the presence of Mg^{2+} (Figure 1A) the degree of adhesion was inhibited ~ 2.5-fold with 100% EDC/NHS crosslinking. Integrin-dependent adhesion is sensitive to the depletion of divalent cations from the surrounding media, and so platelets adhesion was measured in the presence of the divalent cation chelator EDTA (Figure 1B). Platelet adhesion increased dose dependently with increased EDC/NHS crosslinking in the presence of EDTA, reaching parity with the degree of adhesion in the presence of Mg^{2+} at 100% EDC/NHS crosslinking. This profile represents loss of native-like adhesion (Mg^{2+}-dependent) which is replaced by non-native adhesion that persists in the presence of EDTA. Irradiation with either 0.42 or 0.96 J/cm^2 did not significantly influence the binding profile in the presence of Mg^{2+} or EDTA. As such, platelet, and by inference integrin $\alpha_2\beta_1$ adhesion to collagen-based materials is predominantly influenced by EDC, but not UV-based crosslinking strategies.

Platelet adhesion was similar with 0.42 J/cm^2 and 0.96 J/cm^2 UV treatments and so 0.42 J/cm^2 was used for all subsequent assays based on reports that this can minimise collagen fragmentation and denaturation [7].

3.2. Influence of EDC/NHS and UV-irradiation on HT1080 cell adhesion and spreading

HT1080 cells contain integrin $\alpha_2\beta_1$ as the sole collagen-binding receptor [33]. As such, we used this model cell line to probe the effect of UV-irradiation on integrin α_2-dependent cell binding to EDC/NHS crosslinked collagen (Figure 2). Consistent with our previous reports, HT1080 cell adhesion to collagen films was highly sensitive to the degree of EDC/NHS crosslinking. Native-like adhesion, in the presence of 5mM Mg^{2+}, was inhibited with EDC/NHS crosslinking concentrations of above 3%. Conversely cation-independent adhesion, in the presence of 5mM EDTA, increased from 0.19±0.01 to 0.41±0.05 with 100% EDC crosslinking. UV-irradiation had a limited impact on HT1080 cell adhesion over EDC/NHS crosslinking alone, with no statistical difference between the UV-irradiated or control non-irradiated films apart from 60% EDC/NHS crosslinking where there was a slight decrease in cell adhesion on UV-irradiated films ($p= 0.044$). The degree of HT1080 cell adhesion in the presence of EDTA was not altered with UV-irradiation. Therefore, these data indicate that UV-irradiation does not modulate integrin $\alpha_2\beta_1$-dependent adhesion, and may be used to supplement low dose EDC/NHS crosslinking to maintain native-like cell adhesion to collagen.

Integrin-binding to ECM proteins can initiate cellular signalling cascades that induce cellular spreading. Therefore, we examined if UV-crosslinking could influence the degree of cell spreading on EDC/NHS crosslinked collagen (Figure 3). It is evident

from the micrographs that HT1080 cells possessed a pronounced phase-dark, spread phenotype on the low-dose EDC/NHS crosslinking conditions but not on 100 % EDC/NHS crosslinked films (Figure 3A). This was not qualitatively different with 0.42 J/cm^2 UV-irradiation. A cell area measurement was undertaken to provide a quantitative assessment of the cell morphology (Figure 3B). This showed that the HT1080 cell area decreased with 100% EDC/NHS crosslinking ($p=0.005$). When the EDC/NHS dose was decreased to 10 % of the standard condition then the cell area showed equivalence with the non-EDC crosslinked control. Exposure to 0.42 J/cm^2 UV did not statistically alter the cell area over the no-UV controls. Therefore UV-irradiation does not appear to influence integrin $\alpha_2\beta_1$-mediated cell adhesion and spreading onto EDC/NHS crosslinked collagen films.

3.3. Integrin I-domain ligation with EDC/NHS and UV-irradiated collagen

The previous results indicate that UV exposure, in combination with low-dose EDC/NHS chemical crosslinking, does not influence cell-associated integrin α_2 binding to collagen. As each cell contains multiple integrins, they cannot probe interaction at the single receptor level. Therefore, we measured the interaction of purified recombinantly expressed I-domains derived from either integrin α_1 or α_2 with collagen, in a cell-free system. Like the cell-based assays, EDC/NHS chemical crosslinking of collagen ablated Mg^{2+} dependent integrin-I-domain binding (Figure 4). This occurred for both integrin α_1 and α_2, however the characteristics of the response was integrin-type specific. Native-like (EDTA-sensitive) adhesion was lost and instead divalent cation-independent (EDTA-insensitive) binding was observed on 100% EDC/NHS crosslinked collagen films. This binding in the presence of EDTA was particularly evident for the integrin α_2-I-domain. Exposure to 0.42 J/cm^2 UV had no statically relevant impact on integrin α_1-

binding (Figure 4A). By contrast UV inhibited integrin α_2-I-domain binding in the presence of Mg^{2+} at EDC/NHS concentrations of 3%, 10% and 60% with p-values of 0.0074, 0.016 and 0.0012 respectively (Figure 4B). This was most pronounced at 3% EDC/NHS where the absorbance decreased from 0.5±0.04 on the no-UV control to 0.31±0.02 with 0.42 J/cm^2 of UV-irradiation. Conversely, cation independent integrin α_2 I-domain adhesion, in the presence of EDTA, was not affected by UV-irradiation of the collagen films. Therefore UV-irradiation can influence integrin-α_2 but not -α_1 adhesion to low-dose EDC/NHS crosslinked collagen materials.

3.4. HT1080 cell proliferation and surface coverage on EDC/NHS and UV irradiated collagen

Integrin ligation with ECM proteins can initiate outside-in cell signalling that controls cellular processes such as cell survival and proliferation [34]. We therefore examined HT1080 cell proliferation (Figure 5) and colonisation (Figure 6). HT1080 cells proliferated on collagen films that had been crosslinked with up to 10% EDC/NHS (Figure 5) where the cell number/field of view increased from ~20 at day 1 up to ~410 at day 4. Conversely, little cell growth was noted on 100% EDC/NHS crosslinked films with the cell count/field of view increasing from 20±4 at day 1 up to 42±9 at day 4. UV exposure did not affect cell proliferation on collagen films crosslinked with all concentrations of EDC/NHS. A small decrease (p=0.03 against no-UV controls) in the cell count was noted on the UV-irradiated 0% EDC/NHS crosslinked films at day 2 with 59±9 cells/field of view compared to 89±2 on the non-UV-irradiated control. This difference was not evident at day 4. Cell colonisation of the collagen-based materials was sensitive to EDC/NHS crosslinking (Figure 6A). After 4 days in culture HT1080 cells covered ~94.3±1.3% of the surface of a non-crosslinked collagen control film. 1%

or 10% EDC/NHS crosslinking did not alter the cell surface coverage with 96.4±2.6 and 97.4±0.2 % surface coverage respectively. By comparison 100% EDC/NHS crosslinking reduced the surface coverage to 16.4±3.9% ($p=0.0085$ against non-crosslinked controls). UV crosslinking had minimal effect over EDC/NHS crosslinking alone. For 0% EDC/NHS crosslinked films, UV exposure caused a small, ~4%, decrease in cell coverage ($p=0.023$ against no-UV controls), however for all other EDC/NHS crosslinking conditions the surface coverage was non-statistically different with or without UV-irradiation. Interestingly phase contrast microscopy (Figure 6B) showed that although the cells occupied a smaller total area on 100% EDC/NHS crosslinked collagen, the cells appeared, qualitatively, larger than on 0% EDC/NHS controls. UV exposure did not influence this cell morphology. This could be due to a number of factors including the lower cell density, altered cell proliferation or attenuated cell migration on the 100% EDC crosslinked collagen. As such these data show that UV exposure of EDC/NHS crosslinked collagen films has minimal impact on the proliferative response of $\alpha_2\beta_1$ containing cells.

4. Discussion

Insoluble collagen I is frequently used to fabricate a wide range of biomaterials [35]. Due to the inherent properties of collagen, these are generally considered to be biocompatible. Despite this, the majority of collagen-based materials require crosslinking to ensure suitable stability and for optimal mechanical properties [36]. For this reason, a variety of crosslinking approaches have been proposed, including chemical and physical treatment [37]. Here we have used the chemical crosslinker EDC which forms amide bonds between primary amines (on lysine side chains) and adjacent carboxylic acid groups (on aspartic acid and glutamic acid residues) [10,13] and UV-induced crosslinking of aromatic groups (on phenylalanine side chains) [22]. This was chosen as UV irradiation can dose-dependently extend the stability of collagen-based materials in aqueous environments, but with minimal effect on the scaffold 3D morphology [21]. It should be noted that a UV dose of 0.42 J/cm^2 for 30 min was ultimately chosen as this minimises potential conformational disruption and fragmentation collagen [7]. The results are summarised in Table 1.

A crosslinking ratio of 5xEDC : 2xNHS : 1xCOO^- group on collagen (termed 100% crosslinking) produces scaffolds with extended degradation kinetics and stiffer mechanical properties [10,13]. Amino acid analysis (Supplementary Figure 1) verified that amino acid content in our material was comparable to the primary amino acid sequence of bovine collagen I, thus ensuring the stoichiometry of the crosslinking reaction. We found that 100% EDC/NHS crosslinking of collagen ablates divalent cation-dependent, integrin-$\alpha_2\beta_1$ dependent [33], HT1080 cell and platelet adhesion, replacing this with non-native, divalent cation-independent binding. This is consistent with previous reports showing that EDC inhibits cation-dependent cell adhesion to

collagen via all four collagen binding integrins, $\alpha_1\beta_1$, $\alpha_2\beta_1$, $\alpha_{10}\beta_1$ and $\alpha_{11}\beta_1$ [20]. This effect was not due to the 75% ethanol solvent used during EDC-crosslinking as immersion in 75% ethanol did not affect HT1080 cell adhesion to our collagen films (Supplementary Figure 2). Both the EDC- and UV-crosslinking conditions were chosen carefully to minimise denaturation of the collagen material whist reacting with the majority of the free amine groups [10]. This was confirmed by ATR-FTIR spectroscopy, showing no gross chemical modifications after EDC- or UV-crosslinking (Supplementary Figure 3). We have previously shown that the root mean square roughness of collagen-based films reduces from ~0.42μm to ~0.35μm and the tensile modulus increases from ~6 Mpa to ~31 MPa after 100% EDC/NHS crosslinking [38]. These changes in the physical properties of the collagen films could alter the cellular response, however, isolated α_2-I-domain binding is similarly sensitive to EDC/NHS crosslinking. As recombinant I-domains bind at the molecular level, this indicates that chemical modification of integrin-binding motifs within collagen imparts a significant contribution to EDC-induced ablation of integrin $\alpha_2\beta_1$-dependent cell binding. As such our data agrees well with the hypothesis that EDC inhibits cell adhesion to collagen by modification of critical carboxylic acid groups within the collagen GxOG*E*R cell-motifs [39]. It therefore appears that there are conflicting crosslinking requirements for the stability (high EDC concentration) versus bioactivity (low EDC concentration) of collagen-based materials. For this reason we explored a secondary UV-crosslinking process as a strategy to supplement very low-dose EDC crosslinking of collagen whilst maintaining integrin binding.

EDC inhibits cell ligation through modification of glutamic acid residues (E) present in all of the integrin-binding Gxx′GEx″ motifs within collagen, whereas UV-induced modification of phenylalanine residues (F) appears less detrimental to platelet and

HT1080 cell adhesion. This could be explained by the differential integrin specificity of the integrin-binding Gxx′GEx″ motifs in collagen I, each with amino acid substitutions at the x position. For example, the high affinity integrin-α_1 and α_2 binding site, G<u>F</u>OG*E*R, in collagen I, contains a UV-susceptible aromatic group on the phenylalanine (F) in the 'x' position. No such UV-susceptible side chain exists in the high affinity integrin-α_1 binding site GLOG*E*R [30] (Figure 7). This is in agreement with the purified integrin I-domain binding results. EDC-induced modification abated the binding of both integrin α_1- and α_2-I-domains, presumably by modification of the E in all of the high-affinity GxOG*E*R motifs. UV-irradiation did not alter the binding of the integrin α_1-I-domain, where binding can still occur through the unmodified high-affinity GLOG*E*R motif. Conversely, integrin α_2-I-domain binding was sensitive to UV-irradiation at EDC crosslinking concentrations of 3% and 10% because the F in the α_2-high-affinity G<u>F</u>OG*E*R motif is susceptible to UV modification. The unmodified GLOG*E*R motif has low affinity for the α_2-I-domain, so cannot compensate for loss of the G<u>F</u>OG*E*R motif, resulting in lower α_2-I-domain adhesion after UV treatment. It is interesting to further postulate the mechanism by which UV-induced modification of the F in G<u>F</u>OG*E*R could inhibit integrin-α_2 binding. A hydrophobic side chain is critical at the x position of GxOG*E*R for integrin binding [40], and so it is conceivable that either 1) UV induced cleavage of the aromatic group may directly decrease the integrin binding affinity for this site or 2) that coupling of the F to an adjacent group may sterically hinder integrin access to the G<u>F</u>OG*E*R motif. Although UV inhibited α_2-I-domain binding, no effect on $\alpha_2\beta_1$-dependent cell adhesion was observed. The I-domain data suggest that this is because UV modifies solely G<u>F</u>OG*E*R and not the other Gxx′G*E*R motifs within collagen I. It is therefore plausible that the other unmodified integrin binding motifs (where x is leucine, arginine, methionine, glutamine or alanine [5]) could be of

sufficient affinity to maintain integrin-mediated cell adhesion. In this case the proportion of ablated sited is below the threshold required to impact on cell adhesion. Although we feel that it would be useful to directly compare recombinant α_1-I-domain binding to α_1-dependent cell adhesion, we did not attempt to study this here. This is because the Rugli, model $\alpha_1\beta_1$-dependent cell line, is of rat origin and we have recently shown that human and rat integrin α_1 possess different collagen binding properties [39].

Integrin engagement with the ECM can induce signalling cascades that control numerous cellular processes [41]. As such, the EDC-sensitivity of both the cell area and proliferative capacity was probably due to the lack of integrin $\alpha_2\beta_1$ signalling. Consistent with the cell adhesion results, only a small decrease in the proliferative response and cell surface coverage was noted when UV treatment was applied to EDC-crosslinked collagen films. Importantly any UV effect on proliferation and surface coverage was limited to irradiation of a 0% EDC crosslinked control, with no effect when combined with 1%, 10% or 100% EDC crosslinking. Overall the effect of UV irradiation was of a markedly lower magnitude than 100% EDC crosslinking. It should be noted that the long-term proliferation assays were conducted in the presence of 10% fetal bovine serum, whereas the short-term cell attachment assays and purified integrin-I-domain binding assays were in the absence of serum. As serum contains potent cell-adhesive molecules that can bridge between the cell and collagen [42,43], we cannot exclude the possible influence of non-direct cellular interactions via these proteins.

Whilst we have clearly shown that UV-induced crosslinking has minimal impact on integrin-α_2-mediated cellular function *in vitro*, the applicability of this approach for scaffold implantation, *in vivo*, is unclear. In particular, analysing macrophage polarisation in response to UV-crosslinked collagen is an important area of future study. In this context, the UV-irradiation parameters; dose, wavelength and accessory

molecules [8], will require careful attention to minimise collagen fragmentation [26,27], and so potential release of pro-inflammatory peptides [28,29], or the formation of pro-inflammatory chemical groups [44].

Accumulatively the data presented here suggest that UV irradiation of low-concentration EDC crosslinked collagen is a useful method to retain sufficient integrin-binding motifs for cell biological activity of collagen-based materials.

5. Conclusions

Despite recent progress, there remains a need for collagen crosslinking strategies that produce sufficient crosslinks to ensure biomaterials stability, whilst retaining the bio-functionality of cell-interactive motifs. In this work we have determined the relative effect that UV-irradiation, in combination with EDC/NHS chemical crosslinking, exerts on integrin-mediated cellular responses to collagen-based materials. UV-irradiation of low-dose EDC crosslinked collagen did not influence integrin-α_1 attachment. Conversely UV-irradiation inhibited integrin-α_2 ligation with collagen, however this caused only minimal loss of integrin-mediated cell adhesion, spreading, proliferation and colonisation of a collagen-based material. Therefore UV-irradiation can be used to supplement a low-dose EDC crosslinking process, mitigating the complete ablation of biofunction that occurs with higher concentrations of EDC. As such we have shown that balancing UV-irradiation, in combination with EDC, allows controlled biological activity of collagen-based materials. Further consideration would be required to determine the UV-irradiation conditions that elicit an acceptable *in vivo* monocyte/macrophage response for tissue engineering applications.

6. Acknowledgements

The authors would like to thank the EPSRC [Fellowship EP/N019938/1], the ERC [Advanced Grant 320598 3D-E] and the British Heart Foundation [Special Project SP/15/7/31561] for providing financial support for this project. DVB was funded by the Peoples Programme of the EU 7th Framework Programme [RAE no: PIIF-GA-2013-624904].

7. Contribution of Authours

Conceived and designed the experiments: DVB, ND, SWH, RWF, SMB, REC. Performed the experiments: DVB. Analyzed the data: DVB, ND, SWH, RWF, SMB, REC. Wrote the paper: DVB, RWF, SMB, REC.

8. References

[1] F.J. O'Brien, Biomaterials & scaffolds for tissue engineering, Mater. Today. 14 (2011) 88–95.

[2] R. Langer, J.P. Vacanti, Tissue engineering., Science. 260 (1993) 920–926.

[3] C.H. Lee, A. Singla, Y. Lee, Biomedical applications of collagen., Int. J. Pharm. 221 (2001) 1–22.

[4] K.E. Kadler, C. Baldock, J. Bella, R.P. Boot-Handford, Collagens at a glance, J. Cell Sci. 120 (2007) 1955–1958.

[5] S. Hamaia, R.W. Farndale, Integrin recognition motifs in the human collagens, Adv. Exp. Med. Biol. 819 (2014) 127–142.

[6] M.G. Haugh, M.J. Jaasma, F.J. O'Brien, The effect of dehydrothermal treatment on the mechanical and structural properties of collagen-GAG scaffolds, J. Biomed. Mater. Res. - Part A. 89 (2009) 363–369.

[7] D.H. Lew, P.H.T. Liu, D.P. Orgill, Optimization of UV cross-linking density for durable and nontoxic collagen GAG dermal substitute, J. Biomed. Mater. Res. - Part B Appl. Biomater. 82 (2007) 51–56.

[8] M.P. Ohan, K.S. Weadock, M.G. Dunn, Synergistic effects of glucose and ultraviolet irradiation on the physical properties of collagen., J. Biomed. Mater. Res. 60 (2002) 384–391.

[9] J.E. Lee, J.C. Park, Y.S. Hwang, J.K. Kim, J.G. Kim, H. Sub, Characterization of UV-irradiated dense/porous collagen membranes: morphology, enzymatic degradation, and mechanical properties., Yonsei Med. J. 42 (2001) 172–179.

[10] N. Davidenko, C.F. Schuster, D.V. Bax, N. Raynal, R.W. Farndale, S.M. Best, R.E. Cameron, Control of crosslinking for tailoring collagen-based scaffolds stability and mechanics, Acta Biomater. 25 (2015) 131–142.

[11] J.S. Pieper, A. Oosterhof, P.J. Dijkstra, J.H. Veerkamp, T.H. Van Kuppevelt, Preparation and characterization of porous crosslinked collagenous matrices containing bioavailable chondroitin sulphate, Biomaterials. 20 (1999) 847–858.

[12] J.S. Pieper, T. Hafmans, J.H. Veerkamp, T.H. Van Kuppevelt, Development of tailor-made collagen-glycosaminoglycan matrices: EDC/NHS crosslinking, and ultrastructural aspects, Biomaterials. 21 (2000) 581–593.

[13] L.H. Olde Damink, P.J. Dijkstra, M.J. van Luyn, P.B. van Wachem, P. Nieuwenhuis, J. Feijen, Cross-linking of dermal sheep collagen using a water-soluble carbodiimide., Biomaterials. 17 (1996) 765–773.

[14] N. Davidenko, J.J. Campbell, E.S. Thian, C.J. Watson, R.E. Cameron, Collagen–hyaluronic acid scaffolds for adipose tissue engineering, Acta Biomater. 6 (2010) 3957–3968.

[15] C.N. Grover, R.E. Cameron, S.M. Best, Investigating the morphological, mechanical and degradation properties of scaffolds comprising collagen, gelatin and elastin for use in soft tissue engineering, J. Mech. Behav. Biomed. Mater. 10 (2012) 62–74.

[16] R.W. Farndale, T. Lisman, D. Bihan, S. Hamaia, C.S. Smerling, N. Pugh, A. Konitsiotis, B. Leitinger, P.G. de Groot, G.E. Jarvis, N. Raynal, Cell–collagen

interactions: the use of peptide Toolkits to investigate collagen–receptor interactions, Biochem. Soc. Trans. 36 (2008) 241–250.

[17] D. Sheppard, The role of integrins in pulmonary fibrosis, Eur. Respir. Rev. 17 (2008) 157–162.

[18] J.D. Humphries, A. Byron, M.J. Humphries, Integrin ligands at a glance, J. Cell Sci. 119 (2006) 3901–3903.

[19] J. Emsley, C.G. Knight, R.W. Farndale, M.J. Barnes, R.C. Liddington, Structural basis of collagen recognition by integrin α2β1, Cell. 101 (2000) 47–56.

[20] D. V. Bax, N. Davidenko, D. Gullberg, S.W. Hamaia, R.W. Farndale, S.M. Best, R.E. Cameron, Fundamental insight into the effect of carbodiimide crosslinking on cellular recognition of collagen-based scaffolds, Acta Biomater. 49 (2017) 218–234.

[21] N. Davidenko, D. V. Bax, C.F. Schuster, R.W. Farndale, S.W. Hamaia, S.M. Best, R.E. Cameron, Optimisation of UV irradiation as a binding site conserving method for crosslinking collagen-based scaffolds, J. Mater. Sci. Mater. Med. 27 (2016) 14.

[22] D. V Bent, E. Hayon, Excited state chemistry of aromatic amino acids and related peptides. II. Phenylalanine., J. Am. Chem. Soc. 97 (1975) 2606–2612.

[23] D. V Bent, E. Hayon, Excited state chemistry of aromatic amino acids and related peptides. I. Tyrosine., J. Am. Chem. Soc. 97 (1975) 2599–2606.

[24] D. V Bent, E. Hayon, Excited state chemistry of aromatic amino acids and related peptides. III. Tryptophan., J. Am. Chem. Soc. 97 (1975) 2612–2619.

[25] Z. Dai, J. Ronholm, Y. Tian, B. Sethi, X. Cao, Sterilization techniques for biodegradable scaffolds in tissue engineering applications, J. Tissue Eng. 7 (2016) 204173141664881.

[26] K.S. Weadock, E.J. Miller, L.D. Bellincampi, J.P. Zawadsky, M.G. Dunn, Physical crosslinking of collagen fibers: Comparison of ultraviolet irradiation and dehydrothermal treatment, J. Biomed. Mater. Res. 29 (1995) 1373–1379.

[27] K.S. Weadock, E.J. Miller, E.L. Keuffel, M.G. Dunn, Effect of physical crosslinking methods on collagen-fiber durability in proteolytic solutions, J. Biomed. Mater. Res. 32 (1996) 221–226.

[28] N.M. Weathington, A.H. van Houwelingen, B.D. Noerager, P.L. Jackson, A.D. Kraneveld, F.S. Galin, G. Folkerts, F.P. Nijkamp, J.E. Blalock, A novel peptide CXCR ligand derived from extracellular matrix degradation during airway inflammation, Nat. Med. 12 (2006) 317–323.

[29] D.L. Laskin, T. Kimura, S. Sakakibara, D.J. Riley, R.A. Berg, Chemotactic activity of collagen-like polypeptides for human peripheral blood neutrophils., J. Leukoc. Biol. 39 (1986) 255–266.

[30] S.W. Hamaia, N. Pugh, N. Raynal, B. Némoz, R. Stone, D. Gullberg, D. Bihan, R.W. Farndale, Mapping of potent and specific binding motifs, GLOGEN and GVOGEA, for integrin α1β1 using collagen toolkits II and III, J. Biol. Chem. 287 (2012) 26019–26028.

[31] R.W. Farndale, D.A. Slatter, P.R.-M. Siljander, G.E. Jarvis, Platelet receptor recognition and cross-talk in collagen-induced activation of platelets, J. Thromb. Haemost. 5 (2007) 220–229.

[32] B.P. Nuyttens, T. Thijs, H. Deckmyn, K. Broos, Platelet adhesion to collagen, Thromb. Res. 127 (2011) S26–S29.

[33] N. Raynal, S.W. Hamaia, P.R.-M. Siljander, B. Maddox, A.R. Peachey, R. Fernandez, L.J. Foley, D.A. Slatter, G.E. Jarvis, R.W. Farndale, Use of synthetic peptides to locate novel integrin alpha2beta1-binding motifs in human collagen III, J. Biol. Chem. 281 (2006) 3821–3831.

[34] P. Moreno-Layseca, C.H. Streuli, Signalling pathways linking integrins with cell cycle progression, Matrix Biol. 34 (2014) 144–153.

[35] A. Sorushanova, L.M. Delgado, Z. Wu, N. Shologu, A. Kshirsagar, R. Raghunath, A.M. Mullen, Y. Bayon, A. Pandit, M. Raghunath, D.I. Zeugolis, The Collagen Suprafamily: From Biosynthesis to Advanced Biomaterial Development., Adv. Mater. (2018) e1801651.

[36] A. Oryan, A. Kamali, A. Moshiri, H. Baharvand, H. Daemi, Chemical crosslinking of biopolymeric scaffolds: Current knowledge and future directions of crosslinked engineered bone scaffolds, Int. J. Biol. Macromol. 107 (2018) 678–688.

[37] X. Yu, C. Tang, S. Xiong, Q. Yuan, Z. Gu, Z. Li, Y. Hu, Modification of Collagen for Biomedical Applications: A Review of Physical and Chemical Methods, Curr. Org. Chem. 20 (2016) 1797–1812.

[38] C.N. Grover, J.H. Gwynne, N. Pugh, S. Hamaia, R.W. Farndale, S.M. Best, R.E. Cameron, Crosslinking and composition influence the surface properties, mechanical stiffness and cell reactivity of collagen-based films, Acta Biomater. 8 (2012) 3080–3090.

[39] N. Davidenko, S. Hamaia, D. V. Bax, J.D. Malcor, C.F. Schuster, D. Gullberg, R.W. Farndale, S.M. Best, R.E. Cameron, Selecting the correct cellular model for assessing of the biological response of collagen-based biomaterials, Acta Biomater. 65 (2018) 88–101.

[40] P.R.-M. Siljander, S. Hamaia, A.R. Peachey, D.A. Slatter, P.A. Smethurst, W.H. Ouwehand, C.G. Knight, R.W. Farndale, Integrin activation state determines selectivity for novel recognition sites in fibrillar collagens, J. Biol. Chem. 279 (2004) 47763–47772.

[41] J.D. Humphries, M.R. Chastney, J.A. Askari, M.J. Humphries, Signal transduction via integrin adhesion complexes, Curr. Opin. Cell Biol. 56 (2019) 14–21.

[42] M.C. Erat, B. Sladek, I.D. Campbell, I. Vakonakis, Structural analysis of collagen type I interactions with human fibronectin reveals a cooperative binding mode., J. Biol. Chem. 288 (2013) 17441–17450.

[43] K. Sano, K. Asanuma-Date, F. Arisaka, S. Hattori, H. Ogawa, Changes in glycosylation of vitronectin modulate multimerization and collagen binding during liver regeneration, Glycobiology. 17 (2007) 784–794.

[44] S. Kamath, D. Bhattacharyya, C. Padukudru, R.B. Timmons, L. Tang, Surface chemistry influences implant-mediated host tissue responses, J. Biomed. Mater. Res. - Part A. 86 (2008) 617–626.

9. Figure Legends

Figure 1: Integrin $\alpha_2\beta_1$-dependent platelet adhesion (y-axis) to insoluble collagen films chemically crosslinked with increasing concentrations of EDC/NHS (x-axis) and subsequently with no UV (cross, solid line), 0.42 J/cm^2 UV (diamond, long-dashed line) or 0.96 J/cm^2 UV (triangle, short dashed line). 100% crosslinking equates to a ratio of 5 EDC : 2 NHS : 1 COO- group on collagen with the ratio of NHS and EDC varied against the COO- groups on collagen for the other concentrations. Platelet adhesion was measured in the presence of 5 mM Mg^{2+} (**A**) or 5 mM EDTA (**B**). *, *** and **** indicate $p \leq 0.05$, $p \leq 0.001$ and $p \leq 0.0001$ respectively in a student's t-test when comparing the data point indicated to the 0% EDC crosslinked values in all cases. Statistical significance is shown for the no-UV values only. Error bars indicate standard deviations (n=4) of the mean.

Figure 2: Integrin $\alpha_2\beta_1$-dependent HT1080 cell adhesion (y-axis) to insoluble collagen films that had been crosslinked with increasing concentrations of EDC/NHS (x-axis) and subsequently treated with no UV (diamond, black line) or 0.42 J/cm^2 UV (triangle, grey line). The EDC/NHS concentration is shown as a % of a molar ratio of 5 EDC : 2 NHS to each COO^- group on collagen (100%). Adhesion was measured in the presence of 5 mM Mg^{2+} (solid marker, solid line) or 5 mM EDTA (open marker, dashed line). N/S and * indicate $p > 0.05$ and $p \leq 0.05$ respectively in a student's t-test comparing no-UV and 0.42 J/cm^2 UV values at each EDC concentration. Error bars indicate standard deviations (n=4) of the mean.

Figure 3: Phase contrast micrographs (**A**) and cell area measurements (**B**) of HT1080 cells on insoluble collagen films that had been crosslinked with increasing

concentrations of EDC/NHS (left to right in **A**, x-axis in **B**) and subsequently exposed to no UV (top panel in **A**, white bars in **B**) or 0.42 J/cm^2 UV (bottom panel in **A**, grey bars in **B**). Measurements were taken 24 hours after cell seeding in complete cell culture media. The area of a round cell is indicated by a black bar in (**B**). The scale bar represents 100 μm in (**A**). N/S and *** indicate $p>0.05$ and $p\leq0.001$ respectively in a student's t-test between the samples indicated. Error bars indicate standard deviations (n=3) of the mean.

Figure 4: Recombinant integrin α_1-I domain (**A**) and α_2-I domain (**B**) adhesion (y-axis) to chemically crosslinked insoluble collagen films with an increasing molar ratio of EDC/NHS to COO^- groups on collagen (x-axis). 100% represents a molar ratio of 5 EDC : 2 NHS for each COO^- group on collagen. The films were either treated with no UV (diamond, black line) or 0.42 J/cm^2 UV (triangle, grey line). Adhesion was measured in presence of 5 mM Mg^{2+} (solid marker, solid line) or 5 mM EDTA (open marker, dashed line). N/S, * and ** indicate $p>0.05$, $p\leq0.05$ and $p\leq0.01$ respectively in a student's t-test comparing the no-UV values to the 0.42 J/cm^2 UV values for each EDC concentration. Statistical difference is shown for the Mg^{2+} values only. Error bars indicate standard deviations (n=3) of the mean.

Figure 5: Effect of EDC/NHS chemical crosslinking in combination with 0.42 J/cm^2 UV exposure on the growth of HT1080 cells in complete media. 100% NHS/EDC (green lines) represents a ratio of 5 EDC : 2 NHS to each COO^- group on collagen which was diluted to 10% (blue line) or 1% (red line) of this concentration. A no NHS/EDC crosslinked collagen control is shown with a black line. Films were subjected to no UV (solid marker, solid line) or 0.42 J/cm^2 UV (open marker, dashed

line). * and ** indicate p≤0.05 and p≤0.01 respectively in a student's t-test between the samples indicated. Error bars indicate standard deviations (n=3) of the mean.

Figure 6: HT1080 cell surface coverage (**A**) and phase contrast micrographs (**B**) after 4 days culture in complete media. Insoluble collagen films were EDC/NHS chemical crosslinked with a ratio of 5 EDC : 2 NHS for each COO^- group on collagen (100%) and dilutions of this EDC/NHS concentration (x-axis in **A**, left to right in **B**). Films were subsequently exposed to no UV (white bars in **A**, top panel in **B**) or 0.42 J/cm^2 UV (grey bar in **A**, bottom panel in **B**). The scale bar represents 100 μm in (**B**). N/S, * and *** indicate p>0.05, p≤0.05 and p≤0.001 respectively in a student's t-test between the samples indicated. Error bars indicate standard deviations (n=3) of the mean.

Figure 7: Schematic representation showing the potential modification of integrin α_1 (blue lines) and α_2 (pink lines) binding sites on collagen I by EDC (red) or UV (green). The collagen α1(I) chain and binding sites are depicted in orange and the α2(I) chain and binding sites are in blue. ++++, ++ and + above the integrin I-domain indicate strong, moderate and weak collagen binding respectively.

Supplementary figure 1 : Representative amino acid content of the collagen I prior to EDC- or UV-crosslinking (black bars). The predicted amino acid content was derived from the primary amino acid sequence of bovine collagen I (grey bars). Threonine, Serine and Methionine are not shown due to small amounts of degradation during analysis. Lysine and Proline are not shown due to post-translational modification.

Supplementary figure 2 : HT1080 cell adhesion (y-axis) to insoluble collagen films that had been treated with 0% or 75% ethanol in aqueous solution (x-axis). Adhesion

was measured in the presence of 5 mM Mg^{2+} (back bar) or 5 mM EDTA (grey bars). N/S indicates p>0.05 in a student's t-test comparing the values indicated. Error bars indicate standard deviations (n=3) of the mean.

Supplementary figure 3 : FTIR-ATR analysis of untreated (**A**), UV-crosslinked (**B**) and 100% EDC/NHS crosslinked (**C**) insoluble collagen films. Collagen-associated amide peaks are; Amide A NH stretch at 3302 cm^{-1}; Amide I C=O stretch at 1634 cm^{-1}; Amide II NH deformation at 1543 cm^{-1}; Amide III NH deformation at 1236 cm^{-1}.

Table 1 : Summary of the effects observed by different assay methods (left column) when collagen-based films were either EDC/NHS-crosslinked alone (centre column) or combined with UV-crosslinking (right column).

Fig. 1

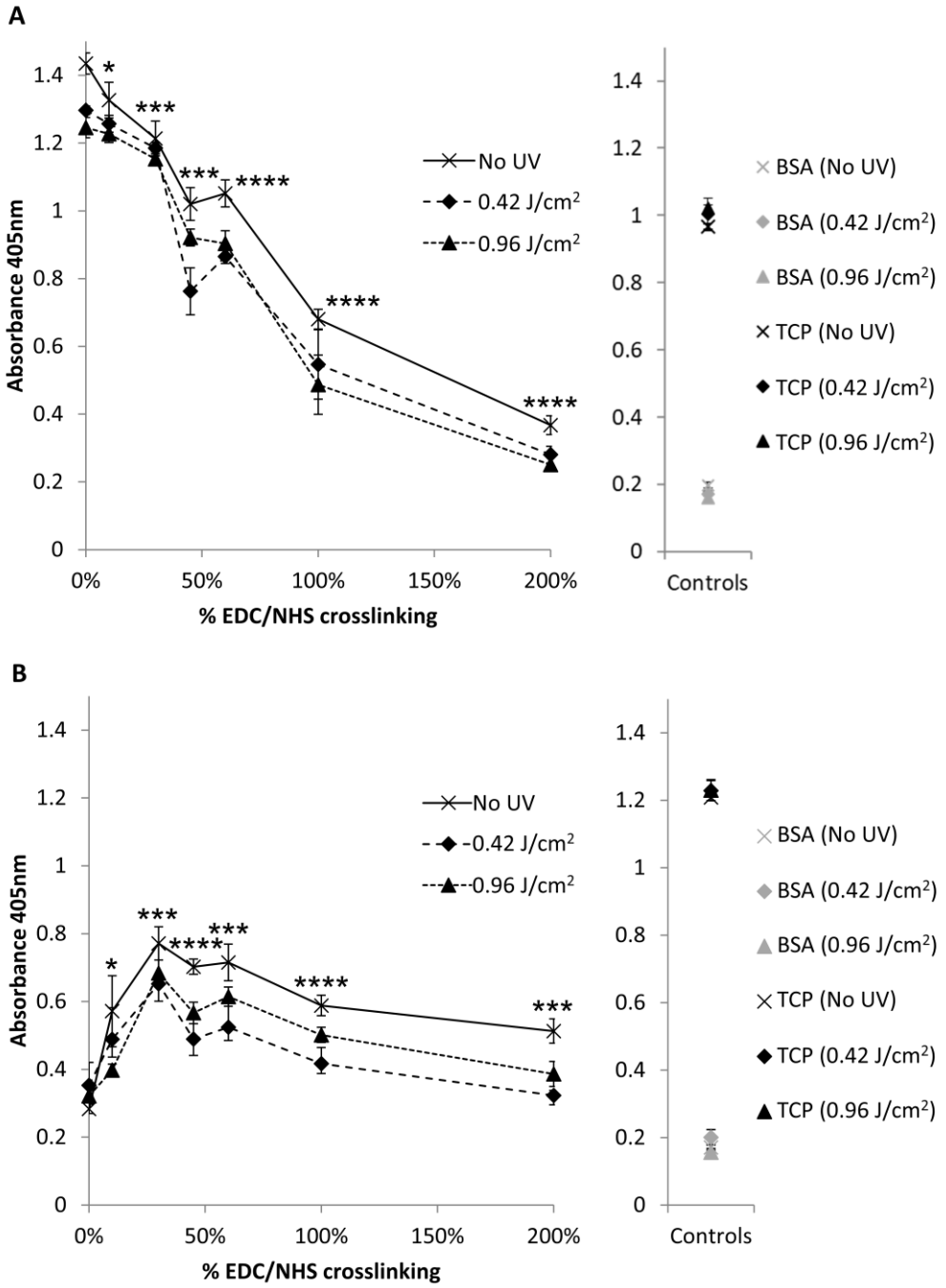
A
Absorbance 405nm
% EDC/NHS crosslinking
0%
50%
100%
150%
200%
Controls
No UV
0.42 J/cm²
0.96 J/cm²
BSA (No UV)
BSA (0.42 J/cm²)
BSA (0.96 J/cm²)
TCP (No UV)
TCP (0.42 J/cm²)
TCP (0.96 J/cm²)
B
Absorbance 405nm
% EDC/NHS crosslinking
Controls
No UV
-0.42 J/cm²
-0.96 J/cm²
BSA (No UV)
BSA (0.42 J/cm²)
BSA (0.96 J/cm²)
TCP (No UV)
TCP (0.42 J/cm²)
TCP (0.96 J/cm²)

Fig. 2

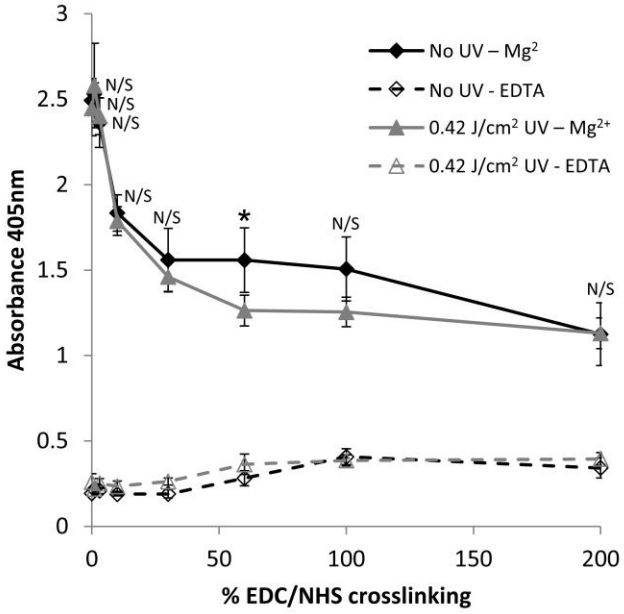
No UV – Mg2
No UV - EDTA
0.42 J/cm2 UV – Mg2+
0.42 J/cm2 UV - EDTA
Absorbance 405nm
% EDC/NHS crosslinking
N/S
*
0
0.5
1
1.5
2
2.5
3
0
50
100
150
200

Fig. 3

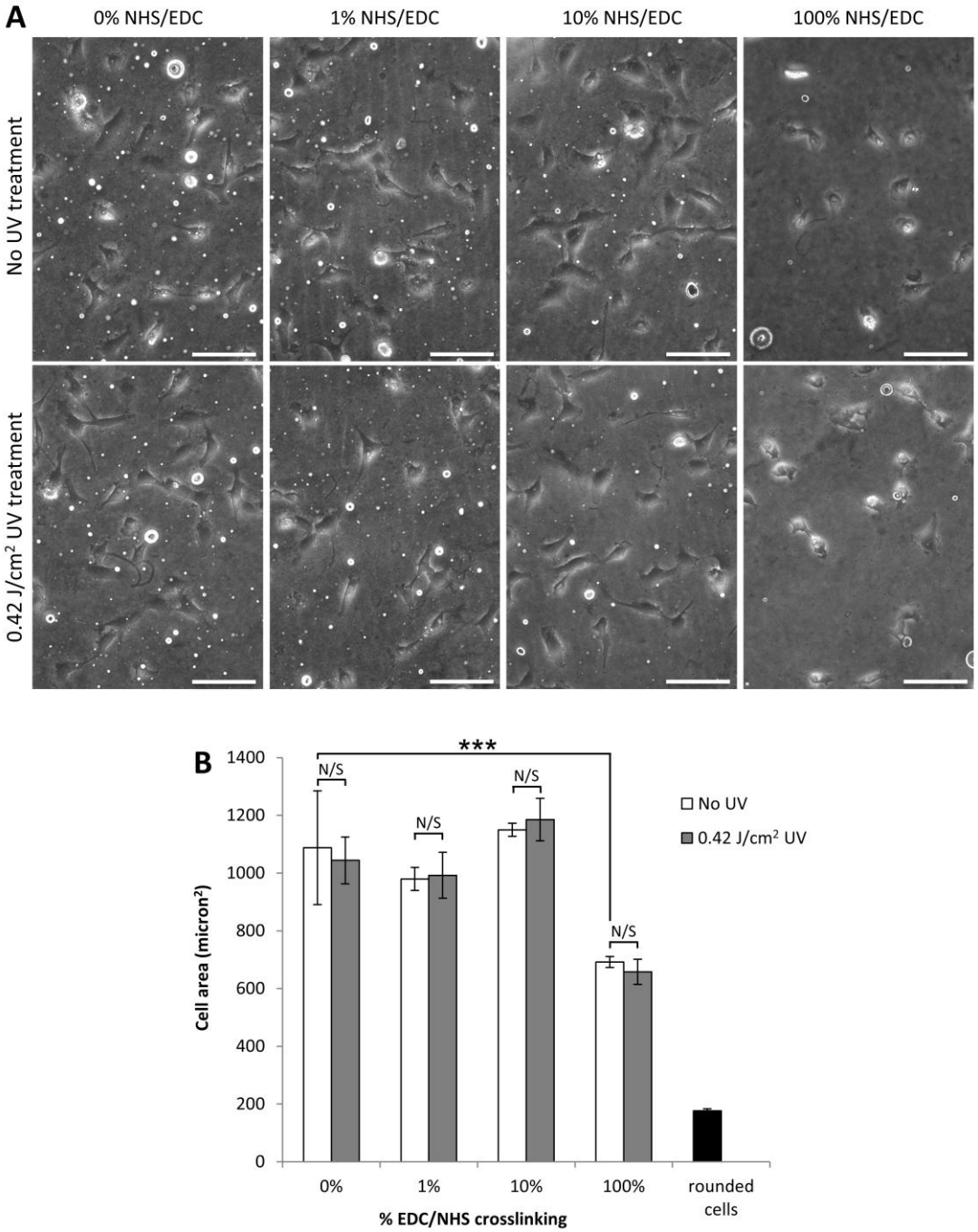
A
0% NHS/EDC
1% NHS/EDC
10% NHS/EDC
100% NHS/EDC
No UV treatment
0.42 J/cm² UV treatment
B
***
N/S
N/S
N/S
N/S
No UV
0.42 J/cm² UV
Cell area (micron²)
1400
1200
1000
800
600
400
200
0
0%
1%
10%
100%
rounded cells
% EDC/NHS crosslinking

Fig. 4

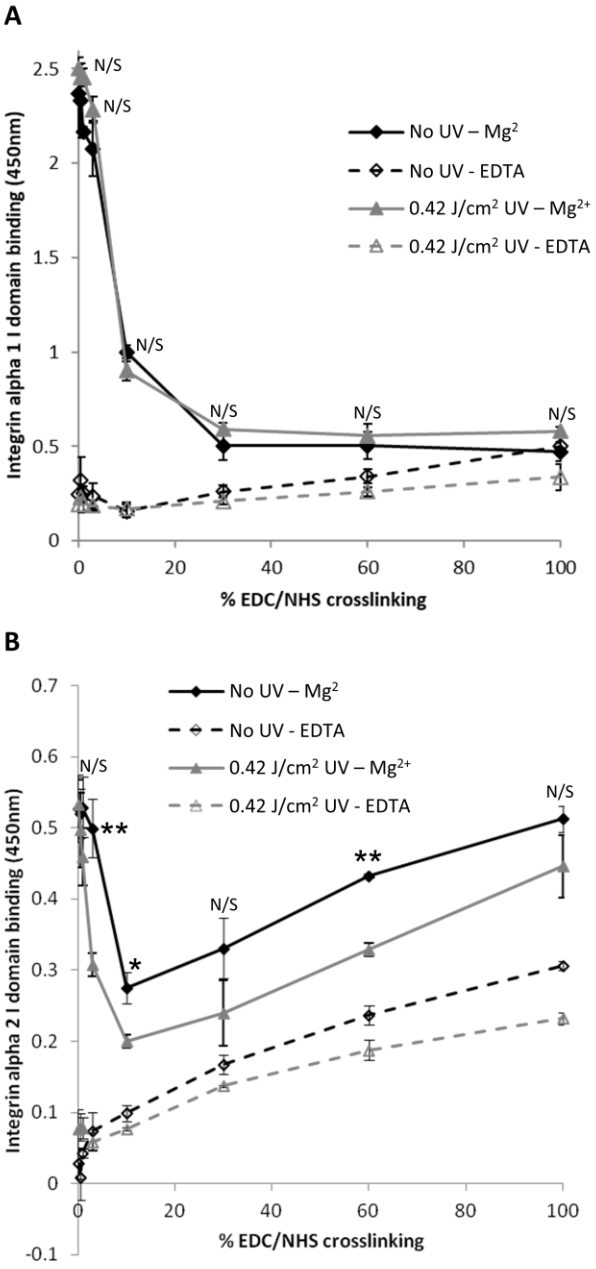
A
Integrin alpha 1 I domain binding (450nm)
% EDC/NHS crosslinking
No UV – Mg2
No UV - EDTA
0.42 J/cm2 UV – Mg2+
0.42 J/cm2 UV - EDTA
N/S
B
Integrin alpha 2 I domain binding (450nm)
% EDC/NHS crosslinking
No UV – Mg2
No UV - EDTA
0.42 J/cm2 UV – Mg2+
0.42 J/cm2 UV - EDTA
N/S
*
**

Fig. 5

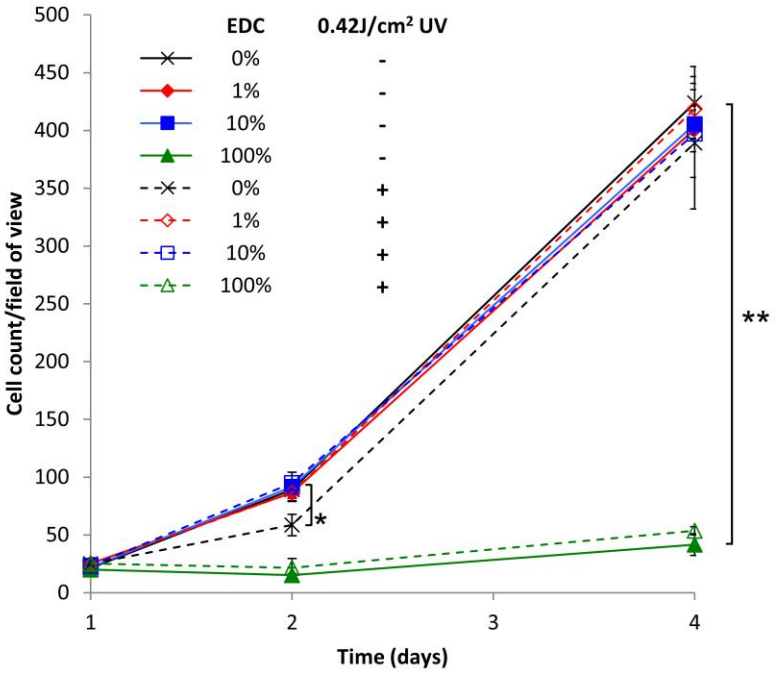
EDC
0.42J/cm² UV
0%
1%
10%
100%
0%
1%
10%
100%
-
-
-
-
+
+
+
+
Cell count/field of view
Time (days)
500
450
400
350
300
250
200
150
100
50
0
1
2
3
4
*
**

Fig. 6

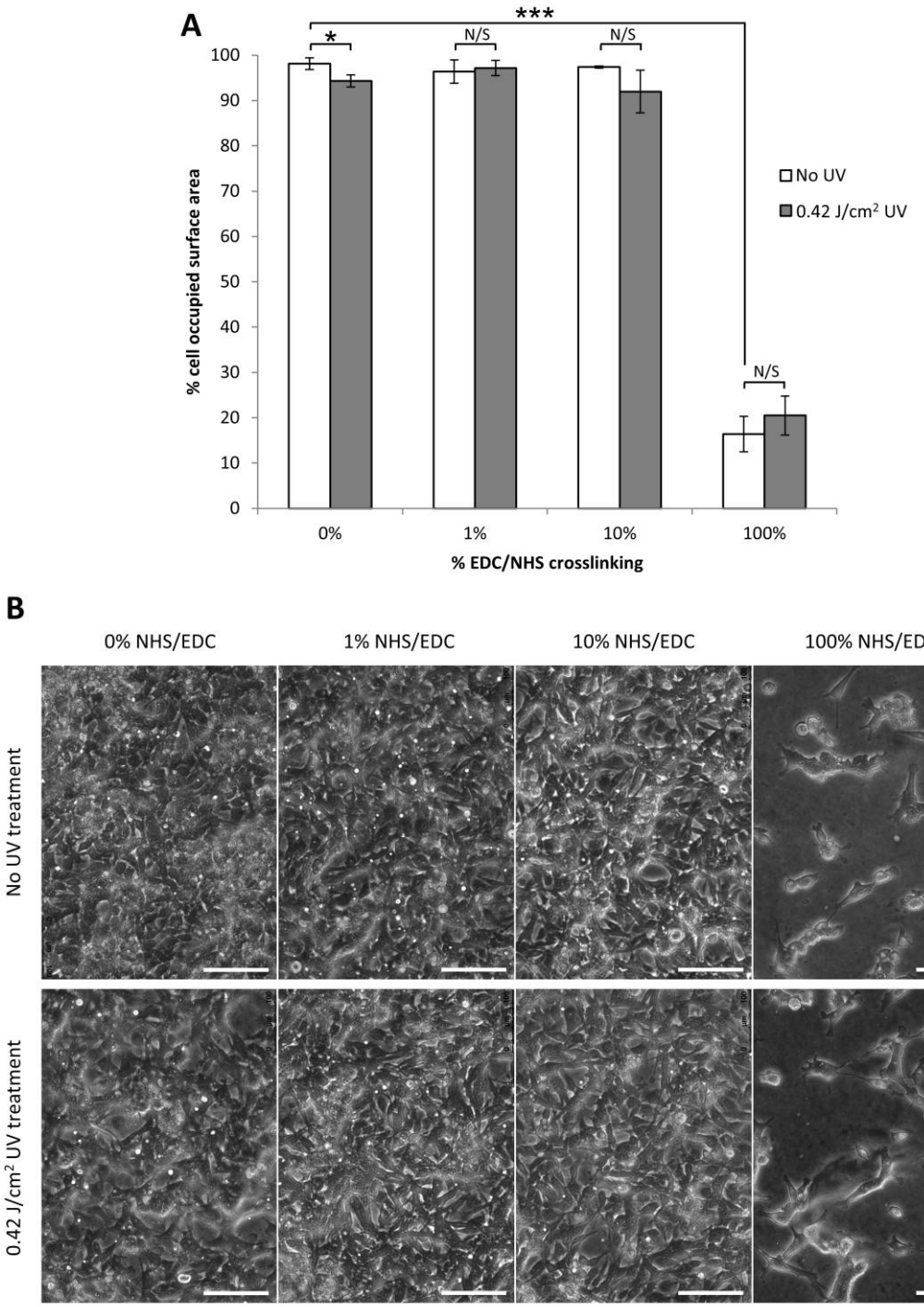
A
***
*
N/S
N/S
N/S
100
90
80
70
60
50
40
30
20
10
0
% cell occupied surface area
No UV
0.42 J/cm² UV
0%
1%
10%
100%
% EDC/NHS crosslinking
B
0% NHS/EDC
1% NHS/EDC
10% NHS/EDC
100% NHS/EDC
No UV treatment
0.42 J/cm² UV treatment

Fig. 7

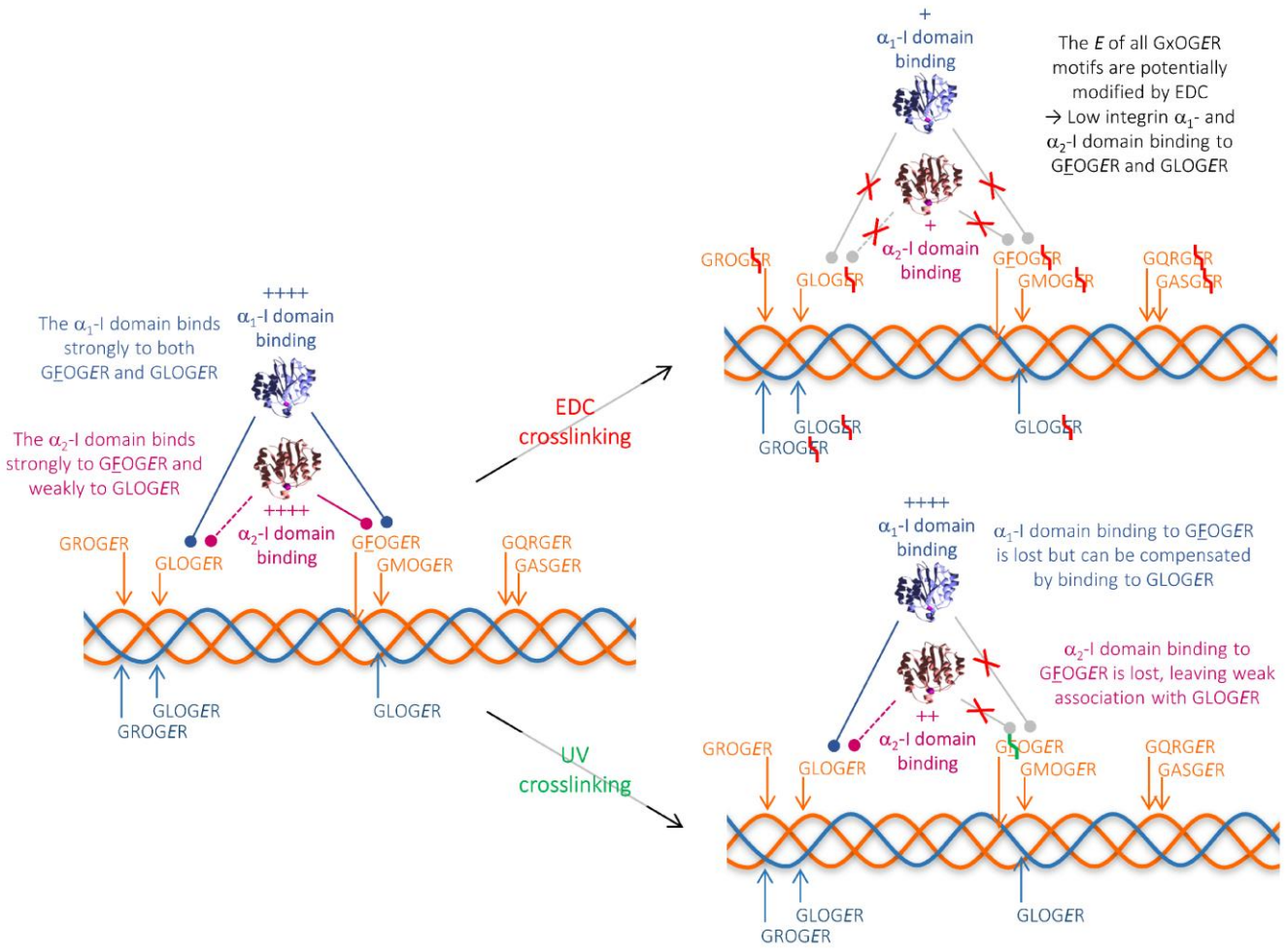
The α_1-I domain binds strongly to both GFOGER and GLOGER
The α_2-I domain binds strongly to GFOGER and weakly to GLOGER
++++
α_1-I domain binding
++++
α_2-I domain binding
GROGER
GLOGER
GFOGER
GMOGER
GQRGER
GASGER
GLOGER
GROGER
GLOGER
EDC crosslinking
UV crosslinking
+
α_1-I domain binding
The E of all GxOGER motifs are potentially modified by EDC
→ Low integrin α_1- and α_2-I domain binding to GFOGER and GLOGER
+
α_2-I domain binding
GROGER
GLOGER
GFOGER
GMOGER
GQRGER
GASGER
GLOGER
GROGER
GLOGER
++++
α_1-I domain binding
α_1-I domain binding to GFOGER is lost but can be compensated by binding to GLOGER
++
α_2-I domain binding
α_2-I domain binding to GFOGER is lost, leaving weak association with GLOGER
GROGER
GLOGER
GFOGER
GMOGER
GQRGER
GASGER
GLOGER
GROGER
GLOGER

Table. 1

Assay Method	EDC effect	UV effect
α_1-I-domain adhesion	Dose dependently inhibits Mg^{2+}-dependent adhesion	No effect
α_2-I-domain adhesion	Dose dependently inhibits Mg^{2+}-dependent adhesion Increases Mg^{2+}-independent adhesion	Inhibits adhesion over EDC alone
Platelet adhesion	Dose dependently inhibits Mg^{2+}-dependent adhesion	Minimal effect
HT1080 cell adhesion	Dose dependently inhibits Mg^{2+}-dependent adhesion Increases Mg^{2+}-independent adhesion	Slight inhibition when combined with 60% EDC
HT1080 cell area	Inhibits spreading at 100% EDC	No effect
HT1080 cell proliferation	Inhibits proliferation at 100% EDC	Minimal effect
HT1080 cell surface coverage	Inhibits surface coverage at 100% EDC	Slight inhibition at 0% EDC

Supplementary Fig. 1

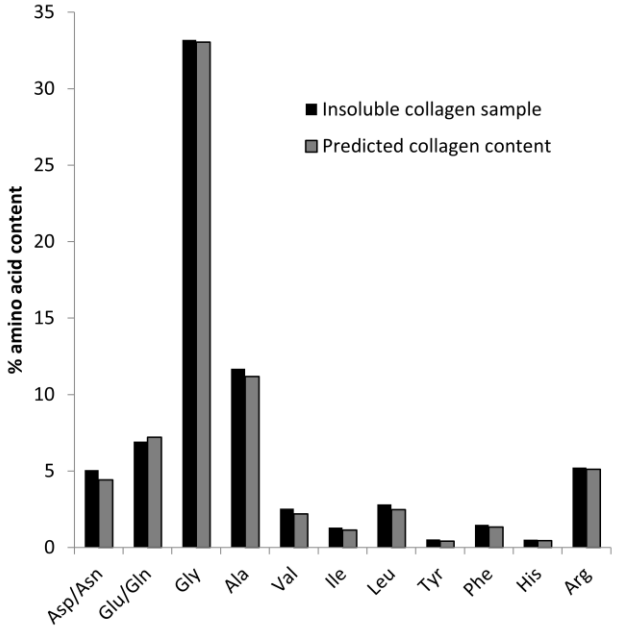

Supplementary Fig. 2

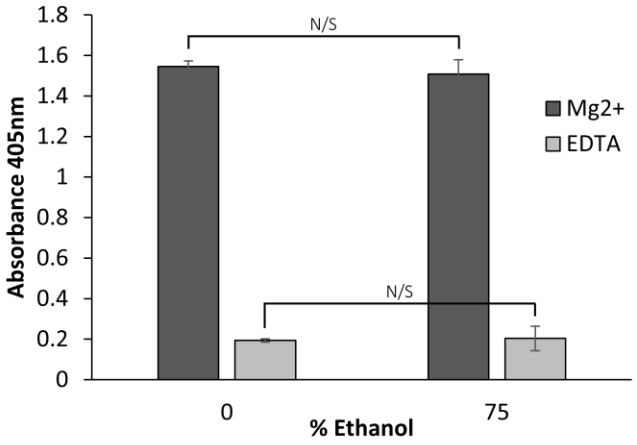

Supplementary Fig. 3